

Dispersive 4-State Kinetic Model for Hole Burning: Bottleneck Effect

In-Ja Lee

Department of Chemistry, College of Natural Science, Dongguk University, Kyongju-si, Kyongpook 780-714, Korea
Received October 29, 1999

The low-temperature physical properties of the amorphous solids such as thermal, acoustic, and dielectric properties largely differ from those of corresponding crystals.¹⁻³ These anomalies are well explained using the two-level system (TLS), which assumes tunneling or thermal activation process of groups of atoms of the amorphous network between equivalent sites.^{2,3}

Nonphotochemical hole burning (NPHB) does not require photoreactivity of the guest molecule but requires the structural rearrangement of the microscopic host configuration around the guest induced by electronic excitation of the guest. Since Hayes and Small applied the TLS model to explain the mechanism of NPHB in 1978,⁴ several hole burning (HB) models have been reported.⁵⁻⁹ Recently, we developed the 3-state NPHB model, which is combined with dispersive kinetics and mean phonon frequency approximation, to explain the hole spectra at arbitrary burn intensities.⁶ Although this model well explains the NPHB hole growth curves and the constant fluence data obtained for the low burn intensities ($\leq 10 \mu\text{W}/\text{cm}^2$), it has difficulties in explaining the constant fluence curves obtained for the high burn intensities.

In this paper, we introduce the 4-state NPHB model to describe the experimental constant fluence curves obtained for the high burn intensity.

Figure 1 represents a simple 4-state NPHB model which is developed to explain the behavior of the constant burn fluence curve. By the photon absorption the system is excited from the ground state $|S_0\rangle$ to the first excited singlet state $|S_1\rangle$ and then experience one of the following pathways: [1] intersystem crossing to the metastable triplet state $|T_1\rangle$ with

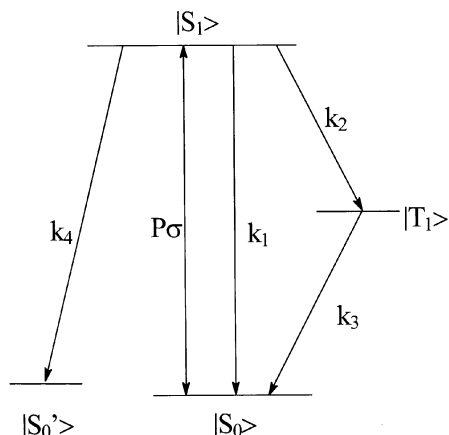


Figure 1. A 4-state NPHB kinetic model. 4-state model consists of the ground state S_0 , excited singlet state S_1 , triplet state T_1 , and hole state S_0 . Hole is produced from S_1 .

rate constant k_2 and then decay back to the ground state with k_3 . The presence of the triplet state is the main difference between the 3-state⁶ and the 4-state NPHB model.; [2] spontaneous and stimulated decay to the ground state with a rate constant k_1 and with rate of $P\sigma$, respectively. Here P is photon flux, σ is absorption cross-section and k_1 includes both radiative and nonradiative contributions; [3] production of hole state $|S_0\rangle$ with k_4 . This step corresponds to the tunneling between the TLS in the excited state followed by the spontaneous decay to the hole state. Because the tunneling process is the rate-determining step, the rate constant is expressed as $k_4 \sim \Omega_0 e^{-2\lambda}$.¹⁰ Here, λ is the tunnel parameter and Ω_0 depends on the TLS deformation potential and asymmetry parameter.¹⁰ Because λ is subject to statistical fluctuations due to the disorder of the matrix, the hole burning is dispersive, too. This model is similar to the ones introduced to explain the bottleneck effect of pentacene,⁷ free-base phthalocyanine⁸ and porphine.⁹ Contrary to our model, those models did not account for the effect of the dispersive kinetics.

In this model, the differential changes of the populations of the ground-, excited-, triplet-, and hole state with time are as follows:

$$\begin{aligned} \frac{dN_0}{dt} &= -P\sigma N_0 + (P\sigma + k_1)N_1 + k_3N_2 \\ \frac{dN_1}{dt} &= P\sigma N_0 - (P\sigma + k_1 + k_2 + k_4)N_1 \\ \frac{dN_2}{dt} &= k_2N_1 - k_3N_2 \\ \frac{dN_3}{dt} &= k_4N_1 \end{aligned} \quad (1)$$

where N_0 , N_1 , N_2 and N_3 are the fractional occupation of levels $|S_0\rangle$, $|S_1\rangle$, $|T_1\rangle$ and $|S_0\rangle$. Here the initial conditions are $N_0(0)=1$ and $N_1(0)=N_2(0)=N_3(0)=0$. The time dependent solutions of these equations are obtained using the Laplace transformation technique and theory of partial fractions. In applying this technique, the roots of the third order equation were calculated using Cardan's formula. Because the tunneling process in the hole burning is dispersive, the hole depth can be written as follows;

$$H(t_B) = \frac{1}{\sqrt{2\pi\sigma_2^2}} \int d\lambda N_3(\lambda, t_B) e^{-(\lambda - \lambda_0)^2/2\sigma_2^2} \quad (2)$$

Here, t_B is burn time and $N_3(\lambda, t_B)$ is population of hole state as a function of tunnel parameter and burn time. And λ_0 and

σ_2 are average and standard deviation of the tunnel parameter for the hole burning, respectively.

Figure 2 shows the changes of the relative populations of S_0 , S_1 , T_1 and S_0' during the hole burning process. The curves are simulated using eq. (2) for the burn intensities of 1000 W/cm^2 (Figure 2-(A)) and $1.0 \mu\text{W/cm}^2$ (Figure 2-(B)). These burn intensities correspond to the stimulated absorption rates of $1.29 \times 10^{11} \text{ s}^{-1}$ and $1.29 \times 10^2 \text{ s}^{-1}$, respectively. When the burn intensity is $1.0 \mu\text{W/cm}^2$, the populations of S_1 and T_1 state are negligibly small during the burning process and no bottleneck effect is expected. When the burn intensity is 1000 W/cm^2 , the hole growth is not operative within the lifetime of S_1 state due to the saturation and also in the μs - ms region due to the bottleneck effect caused by the population build-up in the triplet state. These results indicate that not only photochemical hole burning (PHB) but also NPHB process may be greatly influenced by the bottleneck effect. Therefore, the difficulty of obtaining the deep holes at

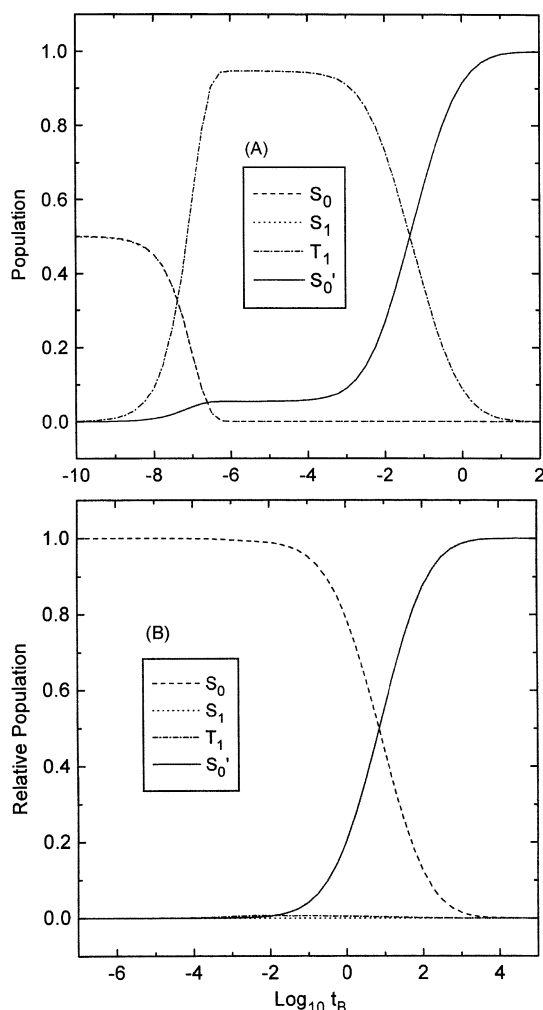


Figure 2. Relative populations of each state as a function of burn time in logarithmic time scale for different burn intensities. The curves are numerically calculated using Eq. (2) and the burn intensities are (A) 1000 W/cm^2 and (B) $1.0 \mu\text{W/cm}^2$, respectively. The populations of S_0 and S_1 state fall on the same curve in (A). The parameter values used are $\lambda_0 = 7.6$, $\sigma_2 = 1.0$, $k_1 = 3.7 \times 10^8 \text{ s}^{-1}$, $k_2 = 1.85 \times 10^7 \text{ s}^{-1}$, $k_3 = 1000 \text{ s}^{-1}$, and $\sigma = 4 \times 10^{-11}$.

short burn times is expected although the very high burn intensity is utilized.

To test the validity of the 4-state NPHB model, the calculated constant burn fluence curves and hole growth curves, which are numerically calculated from the eq. (2) using Bode's approximation, are compared with the experimental results.^{8,10,11} For simplicity, it is assumed in this calculation that the effects of polarization of light and hole filling process are negligible.

Figure 3 represents the hole growth curves of oxazine 720 doped in glycerol host for different burn intensities. The solid lines correspond to the experimental data obtained by Kenney *et al.*¹⁰ for the burn intensities of $I_B = 3.8, 38, 380 \text{ nW/cm}^2$ and the symbols correspond to fit to eq. (2). The coincidence between the experimental and calculated curves indicate that the 4-state NPHB model can successfully explain the behavior of the hole growth curves obtained for low burn intensities in which the bottleneck effect is negligible. For k_1 , λ_0 , σ_2 , σ , and Ω_0 , the same values as those used in the 3-state NPHB model⁶ are utilized in the calculations. From the simulations (not shown), the variations in the k_2 and k_3 , which are related with the triplet state, do negligibly affect the behavior of the hole growth curves for weak burn intensities unless the k_2 is comparable to or larger than k_1 .

For a constant burn fluence (2.2 mJ/cm^2), the hole depths as a function of the burn time are represented in Figure 4. The curve (a) and (b) were calculated to fit the experimental data (symbols), which are obtained for the Oxazine 720 doped in polyvinyl alcohol,¹¹ using 3-state (eq. (2) of ref. 8) and 4-state NPHB model (eq. (2)), respectively. In order to maintain the constant burn fluence, the burn power is adjusted as the burn time is changed. It shows that the hole depths are independent on the burn time for the weak burn

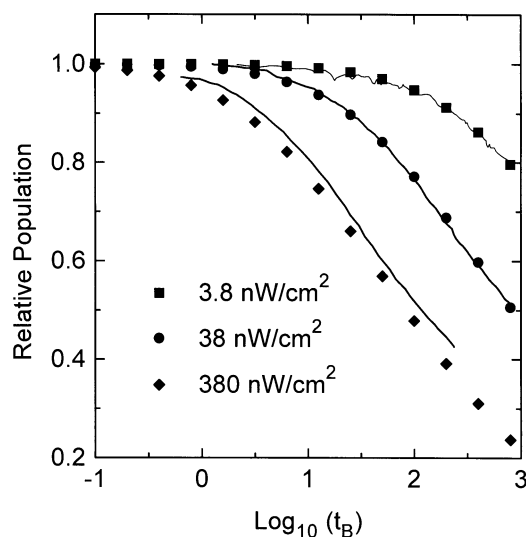


Figure 3. Hole growth curves of Oxazine 720 in glycerol obtained at 1.6 K. The solid curves are experimental data from ref. 10 and the symbols are fits to eq. (2) obtained with $\lambda_0 = 6.8$, $\sigma_2 = 0.8$. The parameter values used are $k_1 = 3.7 \times 10^8 \text{ s}^{-1}$, $k_2 = 1.9 \times 10^7 \text{ s}^{-1}$, $k_3 = 500 \text{ s}^{-1}$, $\sigma = 4.0 \times 10^{-11} \text{ cm}^2$, $S = 0.45$, $\gamma = 1.0 \text{ cm}^{-1}$, $\Gamma = 20 \text{ cm}^{-1}$, and $w_m = 27 \text{ cm}^{-1}$.

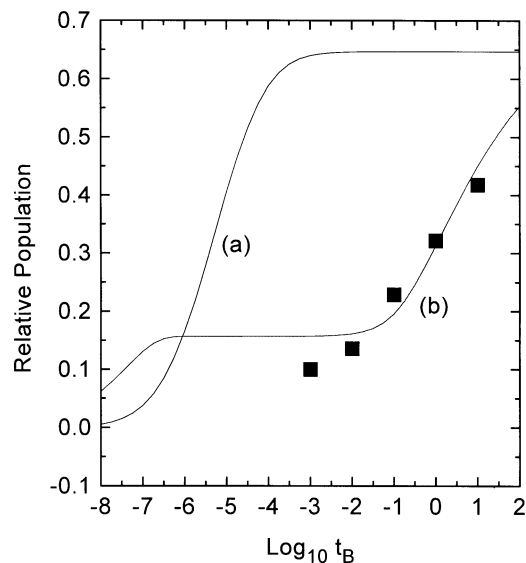


Figure 4. Constant fluence curves (burn fluence = 2.2 mJ/cm^2) of Oxazine 720 doped in polyvinyl alcohol¹¹ at 1.6 K. The solid curves (a) and (b) are calculated for the comparison with the experimental (symbols) using 3-state and 4-state model, respectively. The parameters are $k_1 = 3.7 \times 10^8 \text{ s}^{-1}$, $k_2 = 1.11 \times 10^7 \text{ s}^{-1}$, $k_3 = 10 \text{ s}^{-1}$, $\lambda_0 = 7.2$, $\sigma_2 = 2.0$ and $\sigma = 4.0 \times 10^{-11} \text{ cm}^2$.

intensities while they drop with the burn time over several decades for the relatively higher burn intensities. The curve (a) leans to the left compared with the experimental data. Because all the parameter values related with the states used in the 3-state model is already known,⁶ there is no way that could shift the position of the curve to the right. Because the saturation effect is related with S_0 and S_1 and the bottleneck effect is related with T_1 , the 3-state NPHB model cannot account for the bottleneck effect. Therefore, the 3-state NPHB model seems to be too simple to account for the experimental observations for the system. Contrary to this, the 4-state NPHB model successfully explains the location of the constant fluence curve. The parameters used in the calculations are given in the figure caption. Only new parameters are triplet lifetime and triplet quantum yield Φ_T . In this calculation, Φ_T was taken as ~ 0.03 which is similar to those (~ 0.04)¹² of cresyl violet and nile blue in ethanol whose structures are similar to Oxazine 720. From the fitting, the triplet lifetime of 100 ms was obtained. Because the lifetimes for the individual triplet sublevels of cresyl violet are $80 \mu\text{s}$, 1.5 ms and 60 ms with the relative population of $4 : 2 : 5$ ¹³ and because the triplet state with longest lifetime dominates the bottleneck effect in the hole burning, 100 ms of the triplet state lifetime for the oxazine 720 does not seem to be unreasonable. It is clear that although Φ_T is as small as 0.03, the hole depth is greatly influenced by the bottleneck effect when the burn intensity is high. The power broadening effect, which is larger in the shorter burn times, seems to be the reason why the calculated hole depths are deeper than those of experimental in $\sim \text{ms}$ region.

Because the only difference between NPHB and PHB is the mechanism of k_4 process, which is at S_1 the molecules

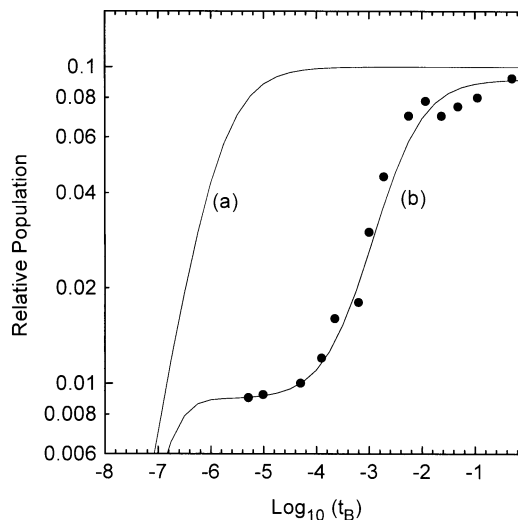


Figure 5. Constant fluence curve (burn fluence = $2.6 \mu\text{J/cm}^2$) of phthalocyanine doped in polyethylene.⁸ The solid curves (a) and (b) were calculated for comparison with the experimental (symbols) using 3-state and 4-state model, respectively. The parameters used are $k_1 = 1.667 \times 10^8 \text{ s}^{-1}$, $k_2 = 1.667 \times 10^7 \text{ s}^{-1}$, $k_3 = 3000 \text{ s}^{-1}$, $\lambda_0 = 7.7$, $\sigma_2 = 0.1$ and $\sigma = 1.312 \times 10^{-11} \text{ cm}^2$.

experience tunneling or thermally activated process in NPHB while they chemically react in PHB, it is anticipated that the 4-state NPHB model can be applied to PHB process as well. Figure 5 represents a constant burn fluence curve ($2.6 \mu\text{J/cm}^2$) obtained by Romagnoli *et al.*⁸ for the phthalocyanine whose hole burning mechanism is PHB. The solid lines (a) and (b) are fits to 3-state (eq. (2) of ref. 8) and 4-state NPHB model (eq. (2)), respectively. Because the life time of S_1 state is known to be 6 ,¹⁴ fluorescence quantum yield is 0.9 ,¹⁵ molar absorption coefficient $\epsilon = 1.37 \times 10^5 \text{ cm}^2/\text{mol}$,⁸ and the ratio of the inhomogeneous to homogeneous widths of the phthalocyanine is 2.5×10^4 ,¹⁶ the fitting parameters used in the calculations are $k_1 = 1.667 \times 10^8 \text{ s}^{-1}$, $k_2 = 1.667 \times 10^7 \text{ s}^{-1}$, and $\sigma = 1.312 \times 10^{-11}$. The best fit is obtained with $\lambda_0 = 7.7$, $\sigma_2 = 0.1$ and the triplet lifetime of $330 \mu\text{s}$ which is close to the experimentally measured value of $350 \pm 50 \mu\text{s}$.⁸ As shown in Figure 5, the constant fluence curve is well explained not by 3-state model but by 4-state model. For the burn times between $100 \mu\text{s}$ and 10 ms , the hole depths drop dramatically due to the bottleneck effect while they are insensitive to the burn time at long burn times. Especially, it is interesting that the experimental has two places where the hole depths are independent on the burn time, one at ≤ 100 region and one at long burn time region. According to Figure 2, it is clear that the first one is related with the bottleneck effect of the triplet state and the second one corresponds to the production of the maximum hole depth for the burn fluence of $2.6 \mu\text{J/cm}^2$. This result indicates that although our 4-state model is originally developed for NPHB, it can be applicable to PHB as well. Because the phthalocyanine experience PHB, it is relatively less influenced by the disorder of the matrix and, therefore, the standard deviation of the hole production rate is relatively very small compared to that of Oxazine 720. In the

calculation, the effect of the Huang-Rhys factor ($S = 0.329$)¹⁷ has been considered.

In summary, the 4-state NPHB model combined with dispersive kinetics has been developed to explain NPHB spectra. The model quantitatively well explains the behavior of the hole growth curves and the constant fluence curves obtained by PHB as well as by NPHB. And it shows that the bottleneck effect due to the population build-up in the triplet state may play an important role in NPHB as well.

Acknowledgment. This work was supported by Dongguk University Research Fund, 1999.

References

1. *Persistent Spectral Hole Burning: Science and Applications*; Moerner, W. E., Ed.; Springer-Verlag: Berlin, 1988 and references therein.
 2. Anderson, P. W.; Halperin, B. I.; Varma, C. M. *Phil. Mag.* **1972**, 25, 1.
 3. Phillips, W. A. *J. Low Temp. Phys.* **1972**, 7, 351.
 4. Hayes, J. M.; Small, G. J. *Chem. Phys. Lett.* **1978**, 54, 435.
 5. Friedrich, J.; Haarer, D. *Angew. Chem. Int. Ed. Engl.* **1984**, 23, 113.
 6. Lee, I.-J. *Bull. Korean Chem. Soc.* **1997**, 18, 240.
 7. Walsh, C. A.; Fayer, M. D. *J. Lumin.* **1985**, 1, 341.
 8. Romagnoli, M.; Moerner, W. E.; Schellenberg, F. M.; Levenson, M. D.; Bjorklund, G. C. *J. Opt. Soc. Am. B* **1984**, 1, 341.
 9. de Vries, H.; Wiersma, D. A. *J. Phys. Chem.* **1980**, 72, 1851.
 10. Kenney, M. J.; Jankowiak, R.; Small, G. J. *Chem. Phys.* **1990**, 146, 47.
 11. Lee, I.-J. *Ph.D. Dissertation*; Iowa State University: Ames, Iowa, 1990.
 12. Lessing, H. E.; Richardt, D.; Von Jena, A. *J. Mol. Structure* **1982**, 84, 281.
 13. Littau, K. A.; Fyae, M. D. *Chem. Phys. Lett.* **1991**, 176, 551.
 14. Kosonocky, W. F.; Harrison, S. E. *J. Appl. Phys.* **1966**, 37, 4789.
 15. McVie, J.; Sinclair, R. S.; Truscott, T. G. *J. Chem. Soc. Faraday Trans. 2* **1978**, 74, 1870.
 16. Moerner, W. E. *Proc. Int. Conf. Lasers '83*; 1984.
 17. Kador, L.; Schulte, G.; Harrer, D. *J. Phys. Chem.* **1986**, 90, 1264.
-